Int J Thermophys (2013) 34:575–587
DOI 10.1007/s10765-012-1205-1

Critical Fluctuations of Membranes: Spectroscopy Meets Thermodynamics

U. Kaatze

Received: 27 March 2012 / Accepted: 25 April 2012 / Published online: 19 May 2012

Abstract Broadband ultrasonic spectra (100 kHz to 2 GHz) of aqueous solutions of liposomes from phospholipids without and with cholesterol or with a peptide added are analyzed near the main phase-transition temperatures of the bilayer systems. All spectra reveal a critical term due to domain structure fluctuations and up to three relaxation terms with discrete relaxation times. By analogy with critically demixing binary fluids, the former is evaluated within the framework of the Bhattacharjee–Ferrell dynamic scaling theory. The relaxation rates of fluctuations and the critical amplitudes resulting from this analysis are discussed briefly. Consistency with and differences to critically demixing systems are demonstrated. The terms with discrete relaxation times are related to short-scale liposome deformation, rotational diffusion of phospholipid molecules, and conformational isomerization of alkyl chains within the bilayers, respectively.

Keywords Concentration fluctuations · Critical amplitude · Critical dynamics · Dynamic scaling · Heat capacity · Membranes · Relaxation rate · Ultrasonic spectroscopy

1 Introduction

Biological membranes are multicomponent systems with intricate structure [1–4]. It is now generally accepted that this complex structure is correlated with membrane functions and is thus a vital aspect in life sciences [3,4]. Since, on the other hand, the predominant constituents of biological membranes are flexible and laterally mobile,

U. Kaatze (✉)
Drittes Physikalisches Institut, Georg-August-Universität Göttingen, Friedrich-Hund-Platz1, 37077 Göttingen, Germany
e-mail: uka@physik3.gwdg.de

membrane structures are subject to considerable fluctuations in the conformation of membrane molecules and in their local concentration. Such fluctuations span a challenging time scale, ranging from correlation times of around 10^{-10} s, as for the relaxation time of the structural isomerization of phospholipid alkyl chains [5], up to 10^5 s for the trans-membrane flip-flop of lipid molecules [1]. Within this broad range, relaxation times for various other mechanisms are found, among them correlation times of domain structure fluctuations of the membranes [6].

Domains exist already in comparatively simple single-component phospholipid bilayer systems which are therefore often investigated as models of complicated biomembranes. Despite their simplicity in chemical composition, such phospholipid systems reveal already highly complex features [7,8]. They undergo a thermotropic phase transition at which, correlated with cooperative melting of the lipid hydrocarbon chains, a change from a solid-like ordered (gel) phase to a liquid-like disordered (fluid) phase occurs [9–11]. Hence, this "main" phase transition of bilayers involves a loss of conformational order of alkyl chains as well as a change in the spatial order of molecules. Near the main phase-transition temperature T_m, thermodynamic domain structure fluctuations over vast ranges of sizes, ranging from molecular dimensions to mesoscopic scales [12], occur. Conformationally disordered fluid domains are formed in the ordered gel phase and vice versa. It is believed that such domain structures and their fluctuations are essential in living systems [13–17]. The average domain size, however, is an equilibrium property that may be expressed by the fluctuation correlation length ξ. The correlation length increases significantly when T_m is approached from either side, thus resembling critical behavior. The critical point, however, appears to be anticipated by a first-order phase transition [13].

In recent years it became apparent that broadband ultrasonic spectroscopy offers a valuable tool to investigate bilayer domain structure fluctuations and also other relaxation phenomena, such as the rotational diffusion of phospholipid molecules and the structural isomerization of their alkyl chains [6]. Ultrasonic spectra of lipid bilayer systems have indeed been measured for a long time [18–28] but the available frequency range was often too small to allow for a reliable subdivision in contributions from different relaxations. This paper summarizes results from recent measurements in sufficiently broad frequency ranges [29–32] to show that the bilayer domain structure fluctuations near T_m can be well treated by analogy with concentration fluctuations of demixing binary liquids near their critical temperature [33]. In addition to single-parameter bilayers, those composed of different phospholipids or those with cholesterol or a peptide enclosed in a phospholipid matrix will be considered in view of effects in the domain structure and dynamics. Albeit the focus is the critical domain fluctuations, parameters of the additional non-critical relaxation terms will be also discussed briefly.

2 Experimental

The phospholipids 1,2-dimyristoyl-3-*sn*-phosphocholine (DMPC), 1,2-dipalmitoyl-3-*sn*-phosphocholine (DPPC), and 1,2-dioleoyl-3-*sn*-phosphocholine (DOPC), as well as cholesterol and the peptide alamethicin were used to prepare suspensions of large

unilamellar liposomes in doubly distilled (Millipore) water [29–32] by means of the extrusion method [34]. As verified by quasi-elastic light-scattering measurements, uniform liposomes with small size distribution were obtained [31]. The transition temperatures T_m of the samples were determined by sound velocity measurements utilizing high-resolution cavity resonator techniques [35–37] and also by recording heat-capacity profiles on highly sensitive differential scanning calorimeters [36,37].

Measurements of the ultrasonic attenuation coefficient α as a function of frequency ν have been performed between 100 kHz and 2 GHz using a resonator method at 100 kHz $\leq \nu \leq$ 15 MHz and a pulse-modulated wave transmission method at 7 MHz $\leq \nu \leq$ 2 GHz [29–32]. The experimental error in these measurements was on the order of $\Delta\alpha/\alpha = 0.01$.

3 Results and Analytical Treatment of Ultrasonic Spectra

In the upper part of Fig. 1, the ultrasonic spectrum of a DMPC suspension is shown in the frequency-normalized format and, in the inset, also as frequency-dependent excess attenuation per wavelength,

$$(\alpha\lambda)_{\text{exc}} = \alpha\lambda - B\nu. \tag{1}$$

Here $\lambda = c_s/\nu$ is the wavelength, c_s is the sound velocity, and $B = B'c_s$, where B' is the asymptotic high-frequency part in the α/ν^2 spectra (Fig. 1). The spectra at 28 °C reveal a broad contribution and also two more narrow relative maxima in the $(\alpha\lambda)_{\text{exc}}$ data, as characteristic for Debye-type relaxations with discrete relaxation times. The low frequency part of the broad contribution increases significantly when the temperature approaches $T_m = 24.0$ °C (Fig. 1, inset). Such behavior is also characteristic for critical binary liquids when approaching their demixing point. In addition to this analogy, similarity to spectra of critically demixing liquids, an example is given in the lower part of Fig. 1 that supports the idea that ultrasonic spectra of liposome suspensions near T_m are dominated by a term reflecting critical fluctuations. Ultrasonic attenuation related to critical demixing and also to fluctuations near the van der Waals critical point has stimulated a variety of theoretical models [38–52], based on the conception that the anomalous attenuation results from a time lag in the establishment of long-range correlations of density fluctuations when the system is slightly disturbed by the pressure and temperature variations of the sonic fields. Experimental results are favorably represented by the Bhattacharjee–Ferrell theory ("BF", [46,48]). In conformity with experimental findings, it predicts a very slow decrease of the absorption-per-wavelength spectrum, proportional to $\nu^{-\delta}$, toward high frequencies (Fig. 1). Here $\delta = \alpha_0/(Z\tilde{\nu}) = 0.058$, where α_0 (= 0.11 [53]) and $\tilde{\nu}$ (= 0.63 [54]) are the critical exponents of the specific heat and the fluctuation correlation length, respectively, and Z (= 3.069 [55,56]) is the dynamic scaling exponent. Another favorable feature of the BF model is its availability in analytical form. Hence, for critically demixing liquids, both parameters controlling the critical ultrasonic attenuation can be obtained from independent data: the relaxation rate Γ of order parameter fluctuations is available

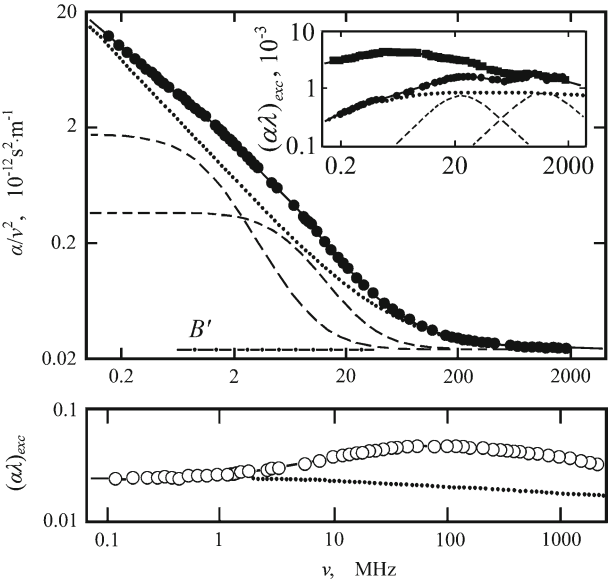

Fig. 1 Top: Ultrasonic attenuation spectrum in the frequency-normalized format for an aqueous solution of liposomes from DMPC (10 mg · ml^{-1}) at 28 °C (•; T_m = 24.0 °C [29]). Inset shows excess attenuation-per-wavelength spectra (Eq. 1) of the solution at the same temperature (•) and also at 24.0 °C(■). Dotted lines are graphs of a Bhattacharjee–Ferrell term, dashed lines show Debye-type relaxation contributions, and dashed-dotted line indicates the asymptotic high-frequency part in the α/ν^2 spectrum. Full lines represent the sum of the relevant terms. Bottom: Ultrasonic excess attenuation-per-wavelength spectrum of the binary isobutoxyethanol—water system of critical composition (○; mass fraction of alkanol $Y = 0.33$, critical temperature T_c = 26.52 °C [58]) at 26.3 °C. Again the BF contribution is represented by a dotted line

from shear-viscosity and dynamic light-scattering measurements and the relaxation amplitude A_{BF} from thermodynamic quantities.

BF dynamic scaling theory has been originally derived to describe critical fluctuations of 3-D binary liquid mixtures. Since the dimensionality is a crucial parameter in the description of critical phenomena, it is not self-evident that the BF model applies also to quasi-2-D domain structure fluctuations of bilayers. However, it has been shown theoretically that the model can be employed to represent the liposome suspension spectra, because fluctuations in the lateral area per molecule are correlated with fluctuations in the local thickness of the membranes [6].

The shape of the experimental spectra of liposome suspensions (Fig. 1) suggests a sum of a BF term and two Debye terms. When evaluating the ultrasonic spectra, however, it turned out that, with some spectra, a meaningful dependence of relaxation parameters upon temperature T requires an additional Debye term at temperatures close to T_m. For that reason, the spectral function,

$$S(\nu, T) = A_{BF}(T) F^*_{BF}(\nu, T) + \sum_{i=0}^{2} \frac{A_i \omega \tau_i}{1 + (\omega \tau_i)^2} + B\nu, \qquad (2)$$

has been used to describe the frequency dependence in the attenuation-per-wavelength data. In this relation $F^*_{\mathrm{BF}}(\nu, T) = \nu^{-\delta} F(\Omega)$, with F denoting the scaling function. $\Omega = \omega/\Gamma$ is the scaled frequency, $\omega = 2\pi\nu$, and the A_i and $\tau_i, i = 0 \ldots 2$, are the amplitudes and relaxation times of the Debye terms, respectively. In the analytical representation of the experimental spectra, the empirical scaling function [57],

$$F(\Omega) = (2/\pi)^{0.5}[\{1 + \Omega^2\}^{0.25} \cos\{0.5 \arctan(\Omega)\} - 1] \tag{3}$$

has been used. Full lines in Fig. 1 are examples to show that Eq. 2 along with Eq. 3 describe the experimental spectra well within the limits of experimental error. Unlike critically demixing systems, the relaxation rate of fluctuations and the critical amplitude are not known from other measurements. Hence, with the liposome solutions, ultrasonic spectroscopy has been applied to determine these parameters of bilayer fluctuations, as will be discussed below.

4 Discussion

4.1 Scaling Function

To verify the appropriateness of relaxation spectral function S, the critical contribution,

$$(\alpha\lambda)_{\mathrm{cr}} = \alpha\lambda - \sum_{i=0}^{2} \frac{A_i \omega \tau_i}{1 + (\omega\tau_i)^2} - B\nu \tag{4}$$

to the attenuation-per-wavelength spectra has been calculated to gain the scaling function according to [33,46,48]

$$F(\Omega) = (\alpha\lambda)_{\mathrm{cr}}(T)/(\alpha\lambda)_{\mathrm{cr}}(T_{\mathrm{m}}). \tag{5}$$

For some bilayer systems such $F(\Omega)$ data, when fitted to Eq. 3, are displayed in Fig. 2. These data were obtained by considering $A_i, \tau_i, i = 0 \ldots 2$, as well as B fixed in the fitting procedure but using Γ as an adjustable parameter.

Both parts of the figure reveal excellent agreement of the experimentally determined $F(\Omega)$ data with the theoretical profile, indicating that the model spectral function (Eq. 2 along with Eq. 3) applies well to the bilayer systems. For single-component bilayers from DMPC, the main part of the figure demonstrates that ultrasonic spectra below and above the transition temperature may be considered. This feature distinguishes the order—disorder transition of single-component bilayers from a demixing point. For DMPC bilayers with 1 % alamethicin added, the inset of Fig. 2 reveals a likewise favorable fit of the experimental data to the theoretical scaling function. No systematic deviations at different temperatures of measurement emerge, indicating again the appropriateness of the spectral function S. Furthermore, the diagram shows that alamethicin does not noticeably affect the scaling function related to the

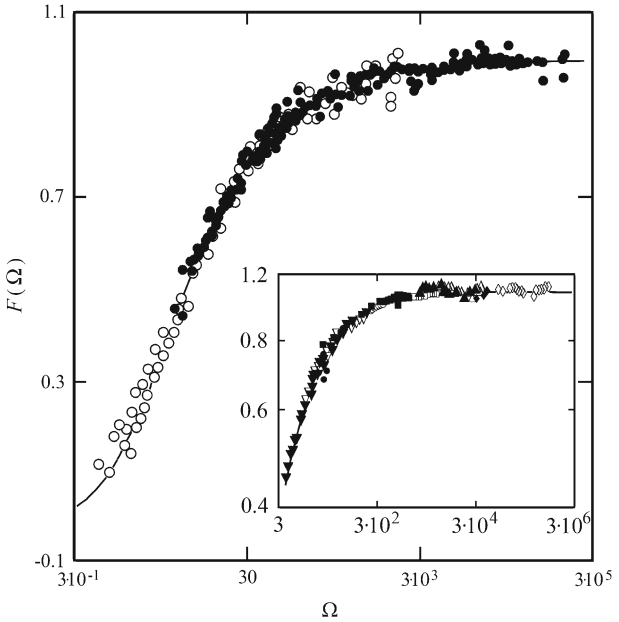

Fig. 2 Lin-log plot of scaling function data (Eq. 5) for a DMPC liposome (10 mg · ml^{-1}) solution in water versus reduced frequency Ω [29]. Data at temperatures below (•) and above (○) T_m are distinguished by symbols. A log–log plot of scaling function data at $T < T_m (= 24.5\,^{\circ}\mathrm{C})$ for DMPC-alamethicin liposomes (99:1 mol· mol $^{-1}$ [30]) is given in the inset. Symbols distinguish measurements at different temperatures between 15 °C(▼) and 23.7 °C(◇)

domain structure fluctuations. At that alamethicin content the peptide molecules cluster already to form pores, accompanied by membrane thinning [37,59–61]. Similar results have been obtained for DMPC bilayers with cholesterol added [32] and for two-component phospholipid bilayers [31] in which, in addition to the conformationally distinct domains, compositionally distinct domains are formed [62]. Effects of bilayer composition are found in the relaxation rate Γ which will be discussed in the next section.

4.2 Relaxation Rate of Fluctuations

Representative examples of relaxation rate behavior are shown in Fig. 5 where Γ values, resulting from the fit of scaling function data (Eq. 5) to the theoretical profile (Eq. 3), are displayed versus T. For each bilayer system the relaxation rate data reveal distinct effects of slowing when T approaches the phase-transition temperature T_m. Close to T_m, the Γ values fall even below the lower limit of the measurement frequency range. Hence, they follow from extrapolation of measured spectra and should thus not be overemphasized.

Often the relaxation rates follow the power law,

$$\Gamma(t) = \Gamma_0 t^{\gamma} \tag{6}$$

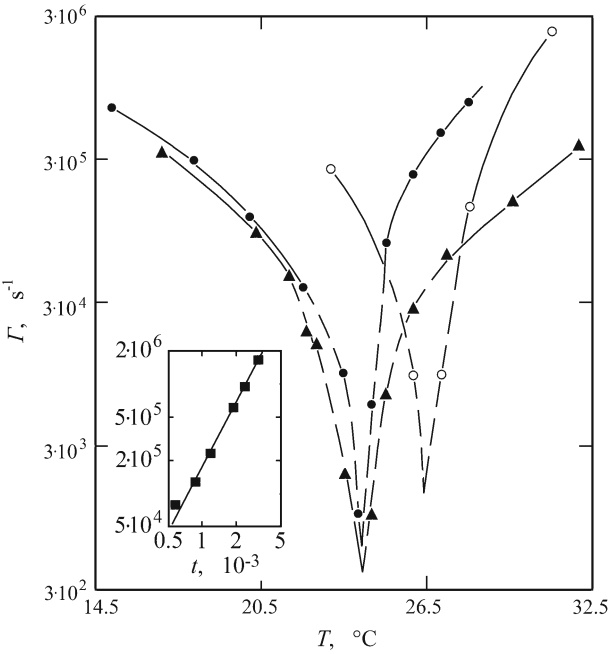

Fig. 3 Relaxation rate Γ of domain structure fluctuations as a function of temperature T for bilayer systems from DMPC (• [29]), DMPC with alamethicin added (▲; 99.3:0.7 mol · mol^{-1} [30]), and a mixture of DMPC and DPPC (○; 83:17 mol · mol^{-1} [31]). Lines are drawn to guide the eye. Dashed lines indicate Γ values corresponding with frequencies below the measurement range. For the DMPC bilayer system at $T > T_m$ the inset shows a log–log plot of Γ values versus reduced temperature t. The line represents a power law (Eq. 6) with universal exponent $\gamma = 1.92$

where $t = |T - T_m| / T_m$ denotes the reduced temperature and Γ_0 is an amplitude. The Γ data for the single-component DMPC bilayer system presented in the inset of Fig. 3 feature even the universal exponent $\gamma = Z\tilde{\nu} = 1.92$ as characteristic for critically demixing binary liquids [33]. Somewhat different γ values, however, have also been found.

Below T_m, the relaxation rates for the fluctuations of the DMPC—alamethicin system almost agree with those of the single-component DMPC bilayers, only at $T > T_m$, a noticeable difference between both series of data emerges. The relaxation rate profiles in the presence of alamethicin are hardly shifted with respect to pure DMPC. This finding is in accordance with sound-velocity profiles for which likewise a minor shift to lower temperatures is observed (Fig. 4). The small reduction in the phase-transition temperature is indicative for a situation in which the peptide does not partition well in both lipid phases. Obviously it forms pores, as mentioned before, or it accumulates at domain interfaces [63]. In contrast, a continuous variation of the main phase-transition temperature, between the limiting values of the pure constituents, is characteristic for binary phospholipid mixtures [64]. For that reason the relaxation rate profile of bilayers from a mixture of DMPC ($T_m \approx 24$ °C) and DPPC ($T_m \approx 41$ °C) is shifted to temperatures above 24 °C (Fig. 3).

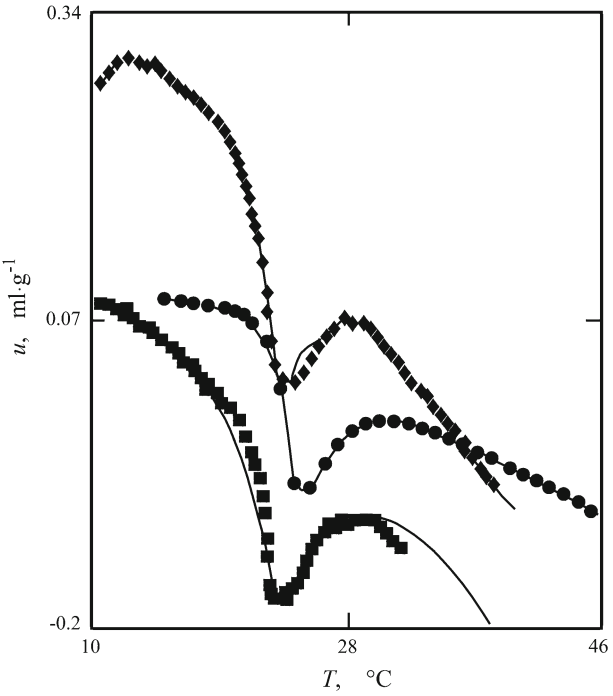

Fig. 4 Sound-velocity number u (Eq. 7) versus temperature T for aqueous suspensions of liposomes from DMPC (• [36]) and mixtures of DMPC with alamethicin (■, 99:1 mol · mol^{-1}; ◇, 98:2 mol · mol^{-1}; [37]). Lines are graphs of the sound-velocity number profiles resulting from heat-capacity profiles

The sound-velocity numbers presented in Fig. 4 are defined by

$$u = (c_s - c_{s0})/(c_{s0}\hat{C}), \tag{7}$$

where c_{s0} is the sound velocity of the solvent and $\hat{C}$ is the solute concentration in mg·ml^{-1}. Here, sound velocities have been used just to determine the main phase-transition temperatures. It is worthwhile to note, however, that the compressibility and heat capacity of membranes are strongly correlated. Based on the experimental findings [65,66] that, close to the melting transition of alkyl chains, volume changes and enthalpy changes of membranes are proportional to each other,

$$\overline{\Delta V}(T) = \beta \cdot \overline{\Delta H}(T), \tag{8}$$

it has been shown that sound-velocity number profiles of bilayer systems can be calculated from heat-capacity traces [36,64,67]. Results of such calculations are shown in Fig. 4 by full lines.

4.3 Critical Amplitude

Different from critically demixing binary liquids, the amplitude A_{BF} of the bilayer systems depends noticeably upon temperature and exhibits a pronounced maximum at the respective T_{m} (Fig. 5). According to the BF theory, the amplitude, according to [33,46,48]

$$A_{\mathrm{BF}}(T) = \frac{\pi \delta C_{pc} c_{\mathrm{s}}(T_{\mathrm{m}})}{2T_{\mathrm{m}} C_{p\mathrm{b}}^2} \left(\frac{\Omega_{1/2} \Gamma_0}{2\pi} \right)^{\delta} g^2(T), \tag{9}$$

can be calculated from thermodynamic parameters, with C_{pc} and $C_{p\mathrm{b}}$ denoting the amplitude of the critical part and the background part of the heat capacity at constant pressure, respectively. In Eq. 9 $\Omega_{1/2}$ is the scaled half-attenuation frequency, $g(T) = \rho(T) C_p(T) \partial T_{\mathrm{m}} / \partial p - T \alpha_p(T)$ is the adiabatic coupling constant, and α_p is the thermal expansion coefficient at constant pressure. Normally, the weakly temperature-dependent first term on the right-hand side dominates the expression for the coupling constant. With bilayer systems, however, the thermal expansion coefficient term exceeds the first term considerably. The thermal expansion coefficient, calculated as the relative slope $\varphi_V^{-1}(T) \mathrm{d}\varphi_V(T)/\mathrm{d}T$ in the temperature dependence of the apparent specific volume φ_V of DMPC, reveals a significant relative maximum at T_{m} (Fig. 5). This maximum certainly contributes to the maximum in the critical amplitudes A_{BF}. It is, however, affected by the opposite effect from the temperature dependence in the background part of the heat capacity. The maximum in the C_p profiles (Fig. 5, inset) are due not only to the critical domain structure fluctuations of the membranes but also to the melting of alkyl chains. The counteracting effect of α_p and $C_{p\mathrm{b}}$ in the BF amplitude may be the reason for the rather broad (when compared to α_p) A_{BF} maxima. Regrettably, the heat-capacity profiles are difficult to analyze in terms of the different contributions, particularly since they display, in addition, a splitting (Fig. 5) which is believed to result from a change of the vesicle geometry during the transition [68].

4.4 Relaxation Times of Non-Critical Terms

In contrast to the relaxation times τ_{diel} from dielectric spectra [69], Debye-term relaxation times τ_1 from ultrasonic spectra reveal noticeable slowing near T_{m} (Fig. 6). Agreement of the order of the τ_1 values with the NMR correlation times for the axial diffusion of phospholipid molecules [5] suggests the ultrasonic relaxation to also reflect the axial diffusion of complete molecules, at variance with the reorientational motions of the dipolar phospholipid head groups which are probed by dielectric spectroscopy [69]. Outside the transition regions, head group reorientations appear to be largely coupled to axial diffusion of the phospholipids. Around T_{m}, the former pass through a step-like change, reflecting the change in the lateral area per head group. The latter are obviously significantly affected by the enhanced fluctuations in the available free volume near T_{m} and thus by a correlation with lateral diffusion.

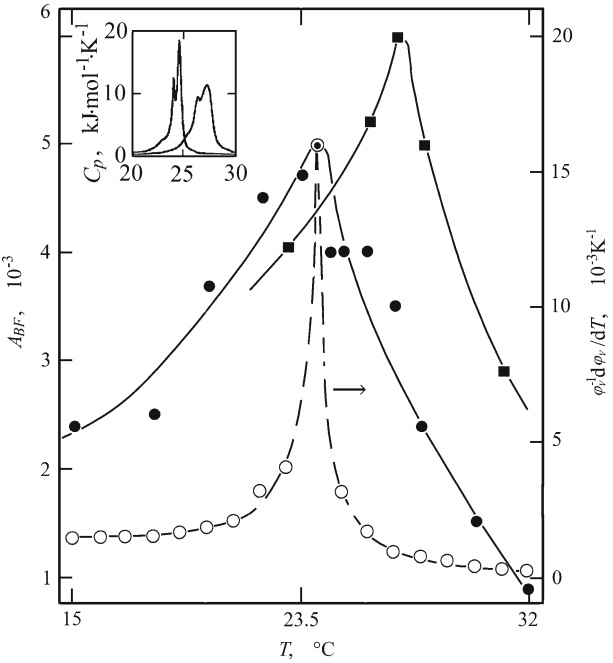

Fig. 5 Critical amplitude A_{BF} (Eq. 9) of sound-velocity spectra as a function of T for liposome solutions from DMPC (•; 10 mg · ml^{-1} [29]) and a mixture of DMPC and DPPC (■; 83:17 mol · mol^{-1} [31], data converted to refer to 10 mg · ml^{-1}). Also given is the thermal expansion coefficient profile for the DMPC system (○). Inset shows heat-capacity traces for both the DMPC and the DMPC–DPPC systems [64]

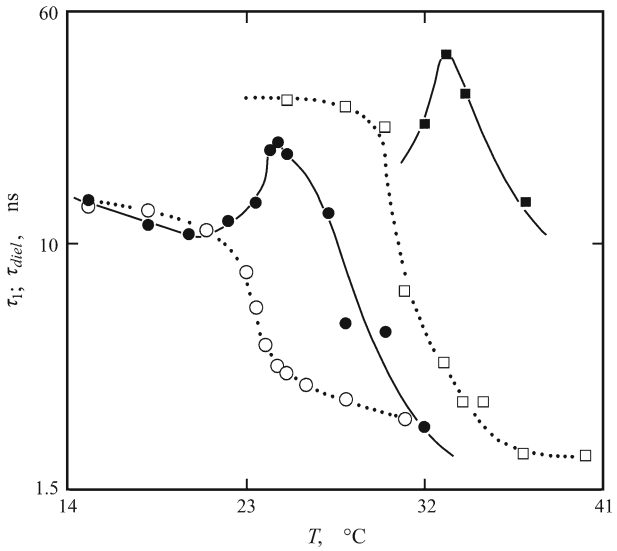

Fig. 6 Relaxation times of Debye-term "1" in the ultrasonic spectra (closed symbols [29,31]) and dielectric relaxation times of the phospholipid head group reorientations (open symbols [69]) versus temperature T for suspensions of liposomes from DMPC (•, ○) and a mixture of DMPC and DPPC (■, □; 50:50 mol·mol^{-1})

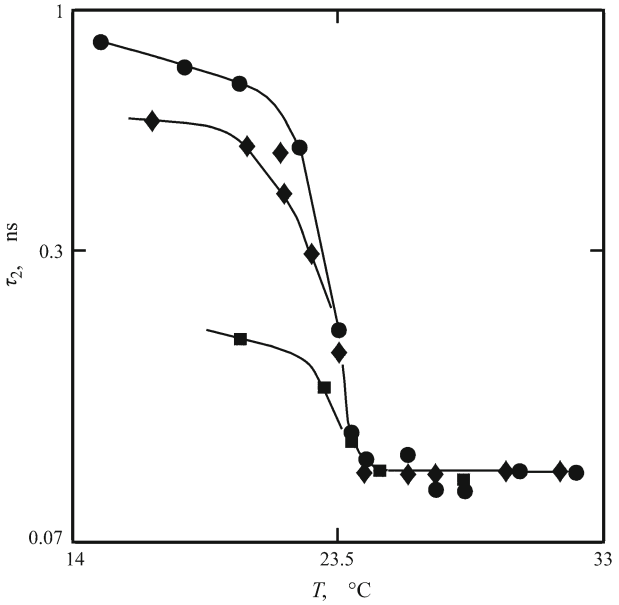

Fig. 7 Relaxation times τ_2 of the high-frequency Debye term in the ultrasonic spectra versus T for liposome aqueous solutions from DMPC (• [29]), and DMPC with alamethicin (◇; 99.3:0.7 mol · mol^{-1} [30]) as well as cholesterol (■; 85:15 mol · mol^{-1} [32]) added

Relaxation times τ_2 of the high-frequency process reveal a distinct step-like change at T_m. The τ_2 values between roughly 100 ps and 1 ns agree with ultrasonic relaxation times of n-alkanes with corresponding lengths [70]. In conformity with results from NMR studies of deuterium-labeled membrane systems [5], they have been assigned to a collective mode of alkyl chain conformational isomerization of the lipids [29] and have been discussed in terms of a torsional oscillator model [71,72]. The step-like change at T_m nicely reflects the enhancement in the mobility of chain structural isomerizations when the bilayers pass the transition from solid-like order to a fluid-like disordered structure (Fig. 7).

Knowledge about the relaxation process with a relaxation time τ_0 (10 ns $\leq \tau_0 \leq$ 170 ns [29,32]) is still incomplete. It has been tentatively assigned to short-scale deformations of the liposome shape in the transition region.

References

1. R.B. Gennis, *Biomembranes, Molecular Structure and Function* (Springer, New York, 1989)
2. O. Sten-Knudsen, *Biological Membranes: Theory of Transport, Potentials and Electrical Impulses* (Cambridge University Press, Cambridge, 2007)

3. R. Lipowsky, E. Sackmann (eds.), *Structure and Dynamics of Membranes: From Cells to Vesicles* (Elsevier, Amsterdam, 1995)
4. T. Heimburg, *Thermal Physics of Membranes* (Wiley, New York, 2007)
5. R.L. Smith, E. Oldfield, Science **225**, 280 (1984)
6. S. Halstenberg, W. Schrader, P. Das, J.K. Bhattacharjee, U. Kaatze, J. Chem. Phys. **12**, 5683 (2003)
7. W.M. Gelbart, A. Ben-Shaul, D. Roux, *Micelles, Membranes, Microemulsions, and Monolayers* (Springer, New York, 1994)
8. K. Larsson, *Lipids—Molecular Organization, Physical Functions, and Technical Applications* (The Oily Press, Dundee, 1994)
9. R.L. Biltonen, J. Chem. Thermodyn. **22**, 1 (1990)
10. W.W. Osdol, M.L. Johnson, Q. Ye, R.L. Biltonen, Biophys. J. **59**, 775 (1991)
11. T. Heimburg, Curr. Opin. Colloid Interface Sci. **5**, 224 (2000)
12. L.K. Nielsen, T. Bjørholm, O.G. Mouritsen, Nature **404**, 352 (2000)
13. R. Zhang, W. Sun, S. Tristam-Nagle, R.L. Headrick, R.M. Suter, J.F. Nagle, Phys. Rev. Lett. **74**, 2832 (1995)
14. K. Jørgensen, O.G. Mouritsen, Thermochim. Acta **328**, 81 (1999)
15. T. Söderlund, A. Jutila, P.K.J. Kinnunen, Biophys. J. **76**, 896 (1999)
16. C. Leidy, W.F. Wolkers, K. Jørgensen, O.G. Mouritsen, J.H. Crowe, Biophys. J. **80**, 1819 (2001)
17. V.V. Volkov, R. Chelli, R. Righini, J. Phys. Chem. B **110**, 1499 (2006)
18. G.G. Hammes, P.B. Roberts, Biochim. Biophys. Acta **203**, 220 (1970)
19. F. Eggers, T. Funck, Naturwissenschaften **63**, 280 (1976)
20. S. Mitaku, A. Ikegami, A. Sakanishi, Biophys. Chem. **8**, 295 (1978)
21. R.C. Gamble, P.R. Schimmel, Proc. Natl. Acad. Sci. USA **75**, 3011 (1978)
22. J.E. Harkness, R.D. White, Biochim. Biophys. Acta **552**, 450 (1979)
23. F.I. Braginskaya, L.Y. Gendel, O.M. Zorina, K.E. Kruglyakova, S.K. Sadykhova, O.A. Serysheva, Sov. Phys. Acoust. **25**, 471 (1979)
24. S.F. Mitaku, T. Date, Biochim. Biophys. Acta **688**, 411 (1982)
25. T. Sano, J. Tanaka, T. Yasunaga, Y. Toyoshima, J. Phys. Chem. **86**, 3013 (1982)
26. S. Mitaku, T. Jippo, R. Kataoka, Biophys. J. **42**, 137 (1983)
27. P.R. Strom-Jensen, R.L. Magin, F. Dunn, Biochim. Biophys. Acta **769**, 179 (1984)
28. R.P.D. Morse, L.D. Ma, R.L. Magin, F. Dunn, Chem. Phys. Lipids **103**, 1 (1999)
29. W. Schrader, S. Halstenberg, R. Behrends, U. Kaatze, J. Phys. Chem. B **107**, 14457 (2003)
30. M. Jäger, Dissertation (Georg-August-Universität Göttingen, Göttingen, 2005)
31. B. Brüning, E. Wald, W. Schrader, R. Behrends, U. Kaatze, Soft Matter **5**, 3340 (2009)
32. W. Schrader, R. Behrends, U. Kaatze, J. Phys. Chem. B **116**, 2446 (2012). doi:10.1021/jp2106007
33. J.K. Bhattacharjee, S.Z. Mirzaev, U. Kaatze, Rep. Prog. Phys. **73**, 066601 (2010)
34. R.C. MacDonald, R.I. MacDonald, B.P.M. Menco, K. Takeshita, N.K. Subbarao, L. Hu, Biochim. Biophys. Acta **1061**, 297 (1991)
35. K. Lautscham, F. Wente, W. Schrader, U. Kaatze, Meas. Sci. Technol. **11**, 1432 (2000)
36. S. Halstenberg, T. Heimburg, T. Hianik, U. Kaatze, R. Krivanek, Biophys. J. **75**, 264 (1998)
37. V. Olinyk, M. Jäger, T. Heimburg, V. Buckin, U. Kaatze, Biophys. Chem. **134**, 168 (2008)
38. M. Fixman, J. Chem. Phys. **33**, 1363 (1960)
39. M. Fixman, J. Chem. Phys. **36**, 961 (1962)
40. K. Kawasaki, Ann. Phys. **61**, 1 (1970)
41. K. Kawasaki, in *Critical Phenomena, Proc. Int. School of Physics "Enrico Fermi"* (Varenna, Italy), ed. by M.S. Green (Academic, New York, 1971)
42. L. Mistura, in *Critical Phenomena, Proc. Int. School of Physics "Enrico Fermi*" (Varenna, Italy), ed. by M.S. Green (Academic, New York, 1971)
43. L. Mistura, J. Chem. Phys. **57**, 2311 (1972)
44. D.M. Kroll, J.M. Ruhland, Phys. Lett. A **80**, 45 (1980)
45. D.M. Kroll, J.M. Ruhland, Phys. Rev. A **23**, 371 (1981)
46. J.K. Bhattacharjee, R.A. Ferrell, Phys. Rev. A **24**, 1643 (1981)
47. K. Kawasaki, Y. Shiwa, Physica A **113**, 27 (1982)
48. R.A. Ferrell, J.K. Bhattacharjee, Phys. Rev. A **31**, 1788 (1985)
49. A. Onuki, J. Phys. Soc. Jpn **66**, 511 (1997)
50. R. Folk, G. Moser, Phys. Rev. E **57**, 683 (1998)
51. R. Folk, G. Moser, Phys. Rev. E **57**, 705 (1998)

52. A. Onuki, Phys. Rev. E **55**, 403 (1997)
53. A.J. Lui, M.E. Fisher, Physica A **156**, 35 (1989)
54. P.C. Hohenberg, B.I. Halperin, Rev. Mod. Phys. **49**, 435 (1977)
55. R.F. Berg, M.R. Moldover, G.A. Zimmerli, Phys. Rev. Lett. **82**, 920 (1999)
56. H. Hao, R.A. Ferrell, J.K. Bhattacharjee, Phys. Rev. E **71**, 021201 (2005)
57. J.K. Bhattacharjee, R.A. Ferrell, Phys. Rev. E **56**, 5549 (1997)
58. K. Menzel, S.Z. Mirzaev, U. Kaatze, Phys. Rev. E **68**, 011501 (2003)
59. M.J. Zuckermann, T. Heimburg, Biophys. J. **81**, 2458 (2001)
60. F.-Y. Chen, M.-T. Lee, H.W. Huang, Biophys. J. **82**, 908 (2002)
61. F.-Y. Chen, M.-T. Lee, H.W. Huang, Biophys. J. **84**, 3751 (2003)
62. B. Cannon, A. Lewis, J. Metze, V. Thiagarajan, M.W. Vaughan, P. Somerharju, J. Virtanen, J. Huang, K.H. Cheng, J. Phys. Chem. B **110**, 6339 (2006)
63. V.P. Iwanowa, I.M. Makarov, T.E. Schäffer, T. Heimburg, Biophys. J. **84**, 2427 (2003)
64. W. Schrader, H. Ebel H., P. Grabitz, E. Hanke, T. Heimburg, M. Hoeckel, M. Kahle, F. Wente, U. Kaatze, J. Phys. Chem. B **106**, 6581 (2002)
65. F.H. Anthony, R.L. Biltonen, E. Freire, Anal. Biochem. **116**, 161 (1981)
66. H. Ebel, P. Grabitz, T. Heimburg, J. Phys. Chem. B **105**, 7353 (2001)
67. T. Heimburg, Biochim. Biophys. Acta **1415**, 147 (1998)
68. M.F. Schneider, D. Marsh, W. Jahn, B. Kloesgen, T. Heimburg, Proc. Natl. Acad. Sci. USA **96**, 14312 (1999)
69. W. Schrader, U. Kaatze, J. Phys. Chem. B **105**, 6266 (2001)
70. R. Behrends, U. Kaatze, J. Phys. Chem. A **104**, 3269 (2000)
71. A.V. Tobolsky, D.B. DuPré, Adv. Polym. Sci. **6**, 103 (1969)
72. M.A. Cochran, P.B. Jones, A.M. North, R.A. Pethrick, J. Chem. Soc., Faraday Trans. II **68**, 1719 (1972)